J. Membrane Biol. 139, 149–165 (1994)

The Journal of
Membrane
Biology

Surface Potentials near the Mouth of the Large-Conductance K^+ Channel from *Chara australis:* A New Method of Testing for Diffusion-limited Ion Flow

D.R. Laver, K.A. Fairley-Grenot
School of Biological Sciences, A12, The University of Sydney, NSW, 2006 Australia

Received: 16 July 1993/Revised: 13 January 1994

Abstract. The kinetics of single K^+ channels were derived for patch-clamp recordings of membrane patches excised from cytoplasmic drops from the plant, *Chara australis* R. Br. Specifically, the "tilt effect" model of MacKinnon, Latorre and Miller (1989. *Biochemistry* **28**:8092–8099) has been used to measure the electrostatic potential (surface PD) and fixed charge at the entrances of the channel. The surface PD is derived from the difference between the trans-pore potential difference (PD) and that between the two bulk phases. The trans-pore PD is probed using three voltage-dependent properties of the channel. These are (1) the association and dissociation rates of Ca^{2+} binding to the channel, from both the cytoplasmic and vacuolar solutions. These were determined from the mean blocked and unblocked durations of the channel in the presence of either 20 mmol liter^{-1} vacuolar or 1 mmol liter^{-1} cytoplasmic Ca^{2+}; (2) the closing rate of the channel's intrinsic gating process. This was determined from the mean channel open time in the absence of vacuolar Ca^{2+} at membrane PDs more negative than -100 mV; and (3) the effect of Mg^{2+} on channel conductance when added to solutions initially containing 3 mmol liter^{-1} KCl.

The voltage dependence of properties 1 and 2 shifts along the voltage axis according to the ionic strength of the bathing media, consistent with the presence of negative charge in the channel vestibules. Furthermore, the magnitude of this shift depends on the current in a manner consistent with diffusion-limited ion flow in the channel (i.e., the rate of ion diffusion in the external electrolyte limits the channel conductance). Mg^{2+} on either side of the membrane alters channel conductance in a voltage-dependent way. A novel feature of the Mg^{2+} effect is that it reverses, from a block to an enhancement, when the membrane PD is more negative than -70 mV. This reversal only appears in solutions of low ionic strength. The attenuating effect is due to voltage-dependent binding of Mg^{2+} within the pore, which presumably plugs the channel. The enhancing effect is due to screening by Mg^{2+} of surface potentials arising from diffusion-limited flow of K^+.

All experimental approaches give a consistent picture of K^+ permeation in which the surface charge and convergence permeability of the cytoplasmic vestibule are the major factors in determining channel conductance. The cytoplasmic vestibule has a charge density of -0.035 C/m^2 which is similar to that found for maxi K channels in rat muscle. The properties of the vacuolar vestibule, which is effectively neutral, differ from the negatively charged external vestibules in rat maxi K channels indicating a differing protein structure in this part of the channel.

Finally, we note that our method of testing for diffusion-limited ion flow, by measuring the dependence of the surface PD on the current passing through the channel, is more reliable than common tests, which make use of nonelectrolytes such as sucrose. It appears that these molecules alter channel conductance by interfering with the intrinsic permeation mechanism of the channel rather than by altering bulk viscosity.

Key words: K^+ channel — *Chara* — Patch clamp — Ion permeation — Surface potential — Diffusion-limited ion flow

Introduction

Two ways in which surface potentials arise at the mouths of ion channels are the nearby presence of

Correspondence to: D.R. Laver, Division of Neuroscience, John Curtin School of Medical Research, Australian National University, ACT, 2601

charged sites on the channel protein or unbalanced mobile charge in the adjacent electrolyte which can arise from nonequilibrium ion concentrations as is the case in diffusion-limited ion flow.

Electrostatic Surface Potentials Arising from Charged Sites

There is now overwhelming evidence from electrical and biochemical studies that ion channel proteins contain charges. These charges arise from amino acids, sialic acid residues and phosphorylation of the protein (Green & Andersen, 1991). They have specific roles in determining the properties of voltage-dependent gating, ligand binding (*see references cited in* Gilbert & Ehrenstein, 1984) and ion permeation (e.g., Imoto et al., 1988). Charged groups located near the pore mouths are also believed to play a nonspecific role in optimizing channel conductance and selectivity by concentrating counter ions within these regions (Apell et al., 1977; Apell, Bamberg & Läuger, 1979; Green & Andersen, 1991). In the case of skeletal muscle, for example, negative charge on both the channel protein (MacKinnon & Miller, 1989) and neighboring lipids (Bell & Miller, 1984; Moczydlowski et al., 1985) are known to enhance K^+ conductance at low ionic strength.

A charged site at the entrance to an ion channel will produce an electrostatic potential that falls off over distance and depends on the electrolyte composition. The resulting potential difference (PD) between the protein surface and the bulk solution is called the surface PD. The surface PD depends on the amount of surface charge and decreases as the ionic strength of the aqueous environment increases. This is due to ion screening, where electrostatic forces near fixed charges cause the mobile ions in the electrolyte to be distributed so they tend to neutralize the fixed charge.

Electrostatic Surface Potentials Arising from Diffusion-Limited Ion Flow

Diffusion-limited ion flow occurs when the diffusion of ions from the bulk solutions to the pore mouths limits the rate of ion transport through the channel. Under these conditions, both the ion concentrations and electrostatic potentials in the vicinity of the pore differ from those in the bulk solutions (Läuger, 1976). Thus, surface PDs can also arise from the flow of ions through a diffusion-limited channel. The magnitude of the surface PD depends on the magnitude of the current and, like surface PD arising from charged sites, decreases with increasing ionic strength.

These properties are used here to provide a novel, reliable method for detecting diffusion-limited ion flow, which measures the dependence of the pore-mouth surface PD on the current. The previous method for detecting diffusion limitation involved measuring the effect on the current of altering the ion diffusion rate outside the pore, by increasing the electrolyte viscosity using nonelectrolytes such as sucrose (Andersen, 1983). This method provided evidence for diffusion-limited ion flow through gramicidin pores (Andersen, 1983) and maxi K channels in *Chara* (Laver, Fairley & Walker, 1989). The disadvantage of Andersen's method is that it requires that the intrinsic conductance of the pore is unaffected by the presence of nonelectrolytes and that the viscosity of the solutions at the entrances to the pore are the same as those of the bulk phases. These conditions have not yet been verified. Furthermore, we find that relating channel conductance to bulk viscosity is a poor test for diffusion-limited ion flow in the *Chara* maxi K channel.

Surface Potentials Can Be Measured Using the "Tilt Effect"

The surface PD at each end of the pore adds to the membrane PD arising from other sources so that the trans-pore PD may differ from that between the bulk phases. Changing the ionic strength on one side of an ion channel will alter the surface PD to produce a "tilt" in the electric potential profile within the pore. This can be seen as a shift in the voltage-dependent kinetics of the channel which is related to the size of the surface PD (*see* Fig. 1 and Theory). One difficulty with this approach is that the screening ions used to alter the surface PD may also block the pore and so alter the channel kinetics by mechanisms other than screening. A method of determining membrane surface charge from the combined ion blocking and screening effects using the tilt-model was discussed by Gilbert and Ehrenstein (1984). An improvement on that experimental approach was made by MacKinnon et al. (1989), who were able to uncouple the ion blocking and screening effects by using a voltage-dependent ion block on one side of the channel to probe the "tilt" in the electric profile produced by the screening effects of ions on the opposite side.

Here, we measure for the *Chara* maxi K channel both the magnitude of the surface charge and diffusion-limited ion flow from the pore mouth surface PDs, using the experimental approaches of Gilbert and Ehrenstein (1984) and MacKinnon et al. (1989). The *Chara* maxi K channel is a large-conductance Ca^{2+}-activated K^+ channel from the vacuolar membrane (tonoplast). The kinetics of this channel has previously been extensively studied as set out in the following paragraph. We use several voltage-dependent characteristics to probe its surface PD. These are (i) the unitary current, i.e., the size of the current steps between the open and

closed states of the channel; (ii) the closing rate of the channel's intrinsic gating mechanism which produces the observed gating kinetics of the channel at membrane PDs more negative than −100 mV. This is one of two voltage-dependent gates which the channel possesses and has been previously referred to as Gate A (Laver & Walker, 1987; Laver, 1990); (iii) the binding rate; and (iv) the unbinding rates of Ca^{2+} from both the cytoplasmic and vacuolar sides of the channel which are measured directly from the Ca^{2+}-induced block of the channel (Laver, 1990, 1992).

Re-evaluating an Ion Permeation Model for the *Chara* K^+ Channel

A model describing the K^+ permeation kinetics of the maxi K channel in *Chara* has been proposed by Laver, Fairley and Walker (1989) in which (i) there is negative surface charge either on the membrane or the protein which significantly increases K^+ conductance for [KCl] up to ~250 mmol liter^{-1}; (ii) saturation of current at high voltages is due to K^+ diffusion external to the pore (diffusion limitation); (iii) ion permeation within the pore is described by electrodiffusion theory; and (iv) only one ion interacts with the pore at any time leading to a [K^+]-dependent, saturating current described by Michaelis-Menten kinetics.

Although the model fitted closely with a broad data set, no direct evidence for negative charge on the *Chara* channel was provided. This study determines whether the channel possesses negative charge of sufficient magnitude to explain the K^+ channel conductance at low ionic strength. This study also re-evaluates the previous permeation model, with particular attention to its tenets concerning surface charge and diffusion limitation.

Materials and Methods

Patch-Clamp and Recording Technique

Details of the patch-pipette fabrication and recording apparatus have been described elsewhere (Laver & Walker, 1987; Laver et al., 1989). Briefly, ion channel currents and pipette potentials were measured with a patch-clamp amplifier (EPC7; List) and recorded on video tape with a bandwidth of 44 kHz using pulse-code-modulation (PCM-501; Sony). Pipette and bath electrodes were made from AgCl-coated Ag wire. The net [Cl^-]-dependent electrode-solution potentials were measured before and after each experiment. In calculating the membrane PDs, account was taken for liquid junction potentials which in these experiments never exceeded ±10 mV (Barry & Lynch, 1991). Here, positive trans-membrane current indicates positive charge flowing from the inside of the membrane.

Recordings of single ion channels were obtained from membrane patches excised from cytoplasmic drops from the plant *C. australis* R. Br. These were formed from internodal cells by the method of Kamiya and Kuroda (1957). During experiments the bath solution usually contained either 150 mmol liter^{-1} NaCl or KCl along with 2 mmol liter^{-1} $CaCl_2$ to enhance the stability of the preparation.

Inside-out membrane patches were made by sealing a fire-polished pipette electrode onto the drop membrane and subsequently withdrawing the pipette. Inside-out patches were preferred to outside-out patches because they were usually more stable and contained fewer channels. The cytoplasmic side of the inside-out patch membrane faces the solution bathing the cytoplasmic drops. To lower the ionic strength of the solution on the cytoplasmic side of these patches, it is necessary to transfer them to a bath separate from that of the drops because cytoplasmic drops are unstable in solutions of low ionic strength. The patch transfer was made using the technique of Quartararo and Barry (1987).

Frequently, nonelectrolytes (300 mmol liter^{-1}) were used in the transfer bath to equalize the osmotic potential with that in the pipette solution. Low ionic strength on the vacuolar side of membrane patches was usually achieved by forming inside-out patches using pipettes filled with solutions of low ionic strength, and occasionally by using the patch transfer method on outside-out patches.

Ca^{2+} and Mg^{2+}used in these experiments were added to solutions as chloride salts. Measurements were carried out over the temperature range 20 to 23°C. All measurements were adjusted to that expected at 23°C using a value of the Q_{10} for conductance of 1.3 (D.R. Laver, *unpublished data*). Theory was fitted to data using a least-squares routine. The errors quoted here represent 95% confidence limits.

Measurement of Open Channel Current

To determine the voltage dependence of the open channel current, membrane patches were subjected to a slowly varying pipette potential which was adjusted manually over the desired voltage range. Recordings of pipette current, filtered at 1 kHz and digitized at 2 kHz, were examined for current transitions using an automated technique described by Laver (1992). Synchronous recording of both the current and membrane PD were analyzed so that the magnitude of current transitions associated with channel opening and closing could be correlated with the membrane PD. In this way, frequency distributions of current transitions were compiled over a range of membrane PDs. The open channel currents were determined from the positions of the peaks in these frequency distributions.

Ion Activity Coefficients

The results were analyzed using ion activity coefficients, γ, which were estimated with the Gouy-Chapman "Limiting Law" (Margolis, 1966).

$$-\log[\gamma] = \frac{0.509 z^2 \sqrt{\mu}}{1 + \sqrt{\mu}} \quad (1)$$

where μ is the ionic strength of the solution in mol liter^{-1} and z is the valency of the ion in question.

Determination of Channel Gating Rates

Voltage-dependent Gate (Gate A)

The maxi K channel is found to possess at least two voltage-dependent gating mechanisms (Laver & Walker, 1987). One of these, referred to as Gate A, is responsible for nearly all of the current tran-

sitions under conditions of low vacuolar [Ca^{2+}] and membrane PDs more negative than −100 mV. Data used to measure the voltage-dependent closing rate of this gate were collected from patches while the pipette potential was clamped to a random sequence of values over the range −250 to −100 mV for periods of 10–100 sec.

Some Ca^{2+} was necessary in the bathing solutions for both patch stability and channel activity. However, it is desirable for these measurements to avoid the presence of Ca^{2+} because its channel blocking and activating properties introduce voltage-dependent gating in addition to that of Gate A (*see below*). Thus, the pipette (vacuolar) solutions usually contained 1 mmol liter^{-1} Ca^{2+} and 150 mmol liter^{-1} KCl. At this concentration, vacuolar Ca^{2+} is sufficient to stabilize the patch and yet have no significant effect on the channel gating. For the cytosolic solutions, it was necessary to include Ca^{2+} because the *Chara* K^+ channel, like other maxi K channels, is activated by cytosolic Ca^{2+} at μmol liter^{-1} concentrations (Laver & Walker, 1991). In these experiments the cytosolic [Ca^{2+}] was kept no less than 1 mmol liter^{-1} so that the Ca^{2+}-dependent gate is mainly open. This has two advantages: channel closures due to the Ca^{2+}-dependent gate are not confused with those of the voltage-dependent gate, and a high [Ca^{2+}] produces longer and more frequent bursts which allows more rapid acquisition of current transitions associated with Gate A. This is particularly useful for measurements at extreme PDs where the membrane patches tend to be less stable. Although cytosolic Ca^{2+} at mmol liter^{-1} concentrations is known to block the channel (*see below*), this is only significant at positive membrane PDs.

The closing rate of Gate A is determined from the mean open time of the channel which is typically less than 3 msec. The protocol for measuring these rapid gating events has been elaborated by Laver and Walker (1987) and Laver (1990). Briefly, frequency distributions of open and closed durations were compiled from single channel recordings filtered at 10 kHz and digitized at 20 kHz (the dead time for event detection is 35 μsec). Software for this (IPROC2) was purchased from Dr. C. Lingle, Department of Biological Sciences, Florida State University. The frequency distribution of open times was found to be a single exponential so that the reciprocal of the mean open time should approximate the closing rate. In calculating the closing rate, allowance was made for the omission of unresolved events using the method of Blatz and Magleby (1986).

Vacuolar Ca^{2+} Block

The gating of the channel is altered by vacuolar Ca^{2+} which enters and plugs the pore (Laver, 1990). The block becomes quite apparent as the membrane PD becomes more negative than −150 mV. The data were collected in the same way as those for Gate A except that the vacuolar solution [Ca^{2+}] was 20 mmol liter^{-1}. Previous analysis of Ca^{2+} block (Laver, 1990) shows that, under these conditions, only a minority of the gating events are due to Gate A so that Ca^{2+} blocking kinetics can be directly measured. It was found that the block produced a 10-fold reduction in the mean open time of the channel and a 10-fold increase in the relative frequency of observed short closures ($t < 1$ msec) in the closed duration frequency distributions. Thus, 90% of the channel closures are Ca^{2+}-induced blocking events. Relatively long channel closures not associated with Ca^{2+} block, though few, have a strong influence on the mean closed time. To exclude the effect of long closures, the mean durations were derived from channel activity within bursts which were defined as groups of channel openings separated by closures exceeding a threshold duration of 10 msec. The reciprocal of the mean open and closed durations within bursts gives a good estimate of the Ca^{2+} association (k^v_{on}) and dissociation rates (k^v_{off}) with the channel protein from the vacuolar side. Here also, when calculating k^v_{off} and k^v_{on}, allowance was made for the omission of unresolved events using the method of Blatz and Magleby (1986).

Cytosolic Ca^{2+} Block

The gating of the channel is also altered by mmol liter^{-1} concentrations of cytosolic Ca^{2+} at positive membrane PD (Laver, 1992). For these measurements, the data were collected over the voltage range 50 to 150 mV and in the presence of 1 mmol liter^{-1} Ca^{2+} in the cytoplasmic bath. The kinetics of Ca^{2+} block from the cytoplasmic side is considerably slower than that from the vacuolar side. The blocking events are manifest as channel closures lasting 10–100 msec which separate bursts of channel activity. Only a minority of the closures are due to Ca^{2+} because the blocking kinetics is relatively slow compared to that of the channel's intrinsic gating mechanism. Although few, these closures are easily recognized because of their long duration. In the present analysis, blocking events are defined as closures exceeding a threshold duration. The threshold is set so that 90% of channel closures exceeding this are Ca^{2+} induced. This is determined by comparing the frequency distributions of closed times in the presence of 1 and 0.1 mmol liter^{-1} cytosolic [Ca^{2+}]. The Ca^{2+} association and dissociation rates are determined from the mean duration of these blocking events, their mean separation and the threshold duration using the method of Blatz and Magleby (1986).

Theory

The theory presented here summarizes how the pore mouth surface PDs are related to both the surface charge density and the ion current through the channel. The superscripts, v and c, indicate parameters associated with the vacuolar and cytoplasmic sides of the channel, respectively. Where the equations apply to both pore entrances, the superscripts are omitted.

The surface PD, Ψ (electrostatic potentials are expressed here in units of RT/F), is defined as the difference between the electrostatic potentials of the bulk phases, Φ, and the pore mouths. Hence the trans-pore PD, U_p is related to the potential difference between the bulk phases (i.e., the membrane PD = $(\Phi^c - \Phi^v)$), by Eq. (2)

$$U_p = (\Phi^c - \Phi^v) + \Psi^c - \Psi^v \tag{2}$$

The relationship between charge density and surface PD depends on the distribution of charged sites at the pore entrances. These distributions are generally unknown for ion channels. Some studies of the charge on membranes and ion channels (Bell & Miller, 1984; Mocydlowski et al., 1985; MacKinnon et al., 1989) related surface PD and charge density by the Gouy-Chapman equation which is only applicable to a charged, infinite plane. This approach has been questioned by other studies (e.g., Dani, 1986) which show that Gouy-Chapman theory is inadequate for charged channel vestibules where the electric field lines have radial symmetry. In any case, the relationship between surface PD and the amount of charge at the pore entrances is by no means

clear. Consequently, the charge densities calculated from surface PDs can only serve as a rough measure of the charged state of the pore vestibules. We have chosen to use the Gouy-Chapman theory so that our results can be directly compared to those obtained from similar studies on maxi K channels in muscle which also use this theory (MacKinnon et al., 1989; MacKinnon & Miller, 1989).

According to this theory, the surface PD at zero current, Ψ_0, is related to the surface charge density, σ, (C/m^2) by Eq. (3) (Grahame, 1947).

$$\frac{\sigma^2}{2\varepsilon_0\varepsilon_r RT} = \sum_{k=1}^{N} c_k(\exp[-z_k\Psi_0] - 1) \tag{3}$$

where c_k and z_k are the bulk concentration and valency of ion species k, respectively, ε_0 is the permittivity of free space and ε_r is the dielectric constant of water.

There is an additional surface PD, Ψ_I when the current is nonzero. Positive current, I, is defined as flowing from the cytoplasmic to the vacuolar side of the membrane. For a neutral cylindrical pore, the dependence of Ψ_I on the current is described by Eq. (4) (Läuger, 1976).

$$\frac{\pm I}{FP_c} = \sum_k c_k(z_k - 1)(1 - \exp[-z_k\Psi_I]) \tag{4}$$

where P_c is the convergence permeability, i.e., the permeability of the electrolyte outside the pore where the current paths converge at each pore mouth. The "±" in Eq. (4) indicates "+" when Eq. (4) is applied to the cytoplasmic solution and "−" when applied to the vacuolar solution. Note that the monovalent cation concentration is not explicity included in Eq. (4), since for these ions the term $z_k - 1 = 0$. However, they are implicity involved via the concentrations of the other ion species since the bulk electrolyte is neutral.

For the case of a charged pore, there is no exact analytical expression for Ψ_I. However, Jordan's (1987) approach to this problem is enlightening: he approximated the effect of charge on diffusion-limited ion flow by multiplying P_c by the Boltzmann factor $\exp[-z\Psi_0]$. Thus, a negative surface charge increases the "effective" convergence permeability of a cation-selective pore. This in turn decreases the dependence of Ψ_I on the current from that predicted by Eq. (4) (*see also* Fig. 7). Here, the surface PD of a charged, diffusion-limited pore is calculated more precisely using numerical methods. Details of the numerical solution to the Nernst-Planck and Poisson flux equations are given in the Appendix.

Inspection of Eqs. (3) and (4) reveals that both current-dependent and current-independent components of Ψ reduce to zero in the limit of high ionic strength. This is a useful property because it allows one to determine experimentally Ψ_0 and Ψ_I from their dependence on ionic strength. At high ionic strength the trans-pore PD is approximately equal to the applied membrane PD because the surface PDs are small. Lowering the ionic strength on one side of the membrane produces a surface PD that offsets the trans-pore PD from the membrane PD (*see* Fig. 1). This offset is manifest as a shift

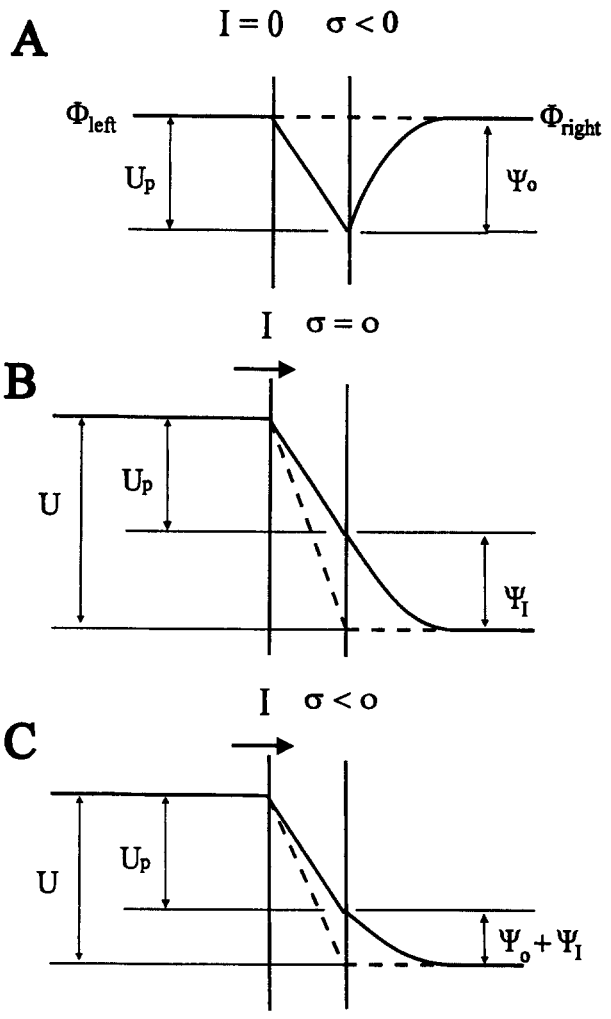

Fig. 1. A schematic of the electrostatic potential profiles in an ion channel and the external aqueous phases. The diagram illustrates how the potential difference across the pore, U_p, differs from that measured at large distances, U. In the example given here, the solution on the left has high ionic strength so that the surface PD on this side is zero. The unbroken lines show the potential profiles when the solution on the right has low ionic strength and the dashed lines show those at high ionic strength. (*A*) When no current flows ($I = 0$) the surface PD, ψ_0 is related to the charge density, σ, by Eq. (3). Raising the ionic strength on the right side reduces ψ_0 to a small value. The trans-pore PD, U_p, is thus made more positive by an amount equal to ψ_0. (*B*) When current flows ($I \neq 0$) through a neutral, ($\sigma = 0$) diffusion-limited pore the surface PD, ψ_I, depends on the current. (*C*) The combined effects of current and negative charge on the surface PD. In this example ψ_I reverses the sign of the surface PD from that shown at zero current in *A*. Here, increasing the ionic strength makes U_p more negative.

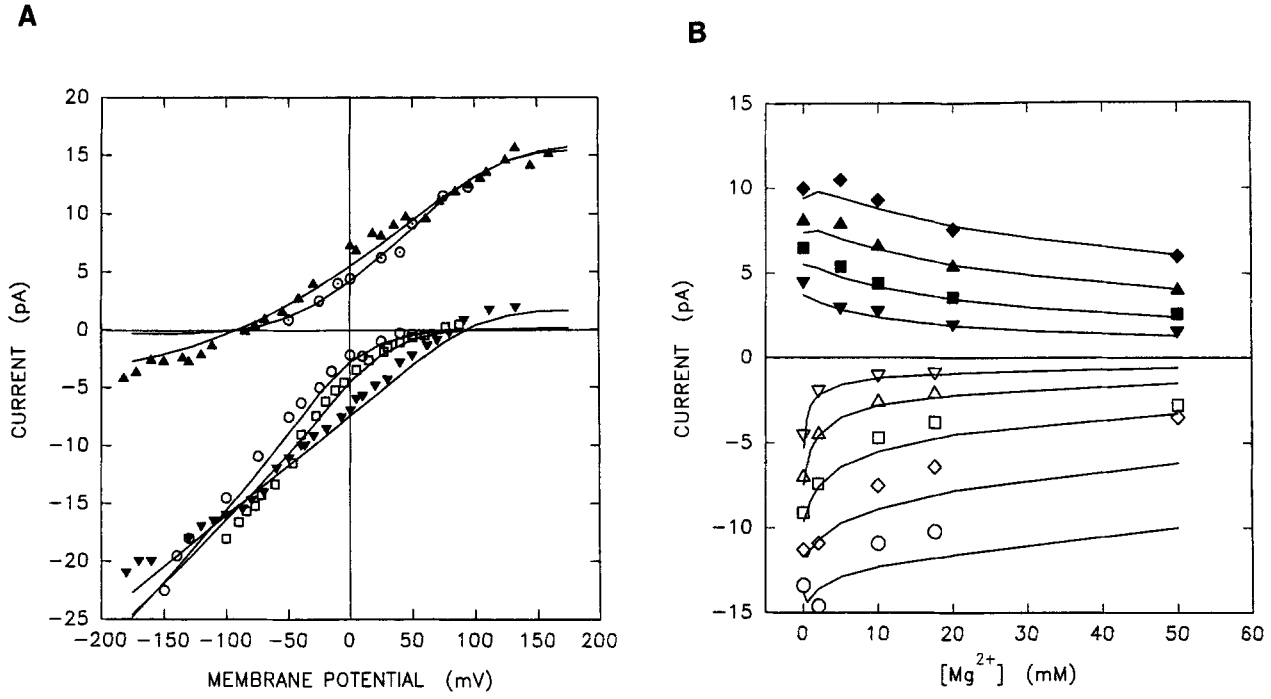

Fig. 2. The effect on the unitary current in excised patches of Mg^{2+} addition to vacuolar and cytoplasmic solutions initially containing 3 mmol $liter^{-1}$ KCl. (*A*) The voltage dependence of the Mg^{2+} effect was measured for $[Mg^{2+}]$ in the range 0–100 mmol $liter^{-1}$. Some of the data are shown here. The unbroken curves are cubic polynomial fits to the data. The solutions on each side of the patch contain (Symbol-vacuolar-; cytoplasmic concentrations (mmol $liter^{-1}$), # number of patches): (▼)-150 KCl; 3 KCl, #3. (□)-150 KCl; 3 KCl + 2 $MgCl_2$, #1. (○)-150 KCl; 3 KCl + 10 $MgCl_2$, #1. (▲) 3 KCl; 150 KCl, #2. (⊙)-3 KCl + 10 $MgCl_2$; 150 KCl, #5. (*B*) The concentration dependence of the Mg^{2+} effect at several membrane PDs obtained from the polynomial fits to the data in (*A*). The filled and open symbols indicate Mg^{2+} addition to the vacuolar and cytoplasmic solutions, respectively. The unbroken curves show the predictions of a K^+ permeation model that includes the effect of surface PDs (*see* Discussion, and Eq. 5). The model parameters are given in Tables 1 and 2. The membrane PD associated with each symbol is: (▼)-25 mV. (■) 0 mV. (▲) 25 mV.
(◆) 50 mV. (▽) 25 mV. (△) 0 mV. (□)-25 mV. (◈)-50 mV. (○)-75 mV.

in the voltage dependence of channel kinetics by an amount which is approximately equal to the surface PD.

Results

The membrane of cytoplasmic drops readily formed 10–50 GΩ seals with fire-polished pipettes. Membrane patches were quite robust and about one-third survived the transition to another bath. It was found that the large osmotic gradient, produced by lowering the ionic strength on one side of the membrane patches, significantly reduced their stability. In most experiments this problem was overcome by introducing nonelectrolytes to equalize the osmotic potentials across the membrane.

Mg^{2+} Effect on Channel Conductance

The voltage dependence of the channel opening and closing current transitions is shown in Fig. 2A, where one side of the membrane is bathed in a solution containing 3 mmol $liter^{-1}$ KCl plus a range of concentrations of the impermeant ion, Mg^{2+}. Nonelectrolytes were not used because they are shown here and elsewhere (Laver et al., 1989) to attenuate the current. Addition of Mg^{2+} to the side of the membrane with low ionic strength had a biphasic effect on the current which is not evident in previous studies of ion block at high ionic strength (Laver, 1992). This biphasic response is shown more clearly in Fig. 2B. At low voltages, both cytoplasmic and vacuolar Mg^{2+} produce a high affinity blocking effect at low concentrations and a lower affinity block which is evident at high concentrations. At more extreme membrane PDs, the high affinity component of the attenuation is replaced with an enhancement of the current.

Voltage-dependent Gating

Figure 3 shows the closing rate, k_c, of the voltage-dependent gate (Gate A) determined from the channel

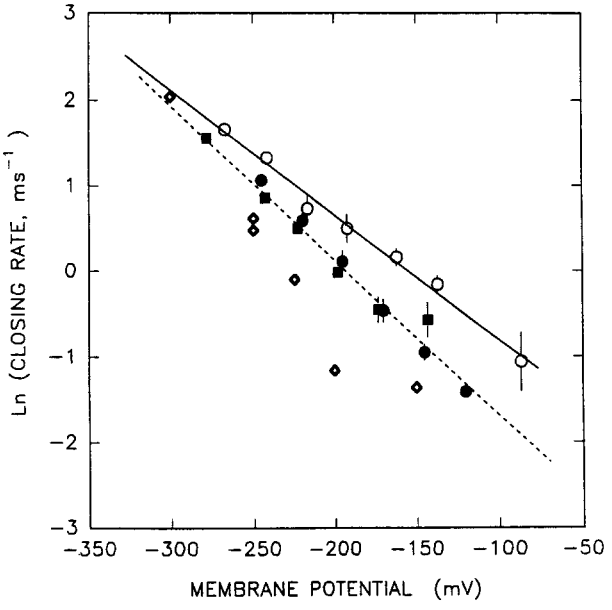

Fig. 3. The voltage dependence of closing rate of the channel's intrinsic gate, Gate A (*see* Introduction) in cytoplasmic solutions of either low or high ionic strength. The closing rate is determined from the channel mean open time from inside-out patches (*see* Materials and Methods). The vacuolar solution contained 150 mmol liter^{-1} KCl + 1 mmol liter^{-1} $CaCl_2$. The cytoplasmic solution contained (Symbol − concentrations (mmol liter^{-1}), # number of patches): (○)-2 $CaCl_2$ + 300 sorbitol, #5. (●)-150 NaCl + 2 or 5 $CaCl_2$, #3. (■)-150 LiCl + 2 $CaCl_2$, #2. (◇)-drop-attached patches. The error bars represent the standard deviations of several measurements. The unbroken line shows the linear least-squares fit to the data obtained at high ionic strength (slope = −18.1 ± 1.4 V^{-1}; intercept = 3.66 ± 0.1). The dashed line shows the fit to the data at low ionic strength (slope = −14.6 ± 1.8 V^{-1}; intercept = −2.20 ± 0.25). There is a significant difference between the slopes of the voltage dependence of channel closing obtained at high and low ionic strength. The lateral shift in the voltage dependence varies from 15 to 38 mV across the experimental voltage range. It is argued in the Discussion that this variation is due to the voltage dependence of the current.

mean open time (*see* Materials and Methods). The voltage dependence of k_c depends on the ionic strength of the solution on the cytoplasmic side. At high ionic strength, the slope of the voltage dependence of k_c is −18.1 ± 1.4 V^{-1}. Decreasing ionic strength from 153 to 6 mmol liter^{-1} significantly (significance of 99.5%, based on the two-sample *t* test) reduced the slope of this voltage dependence to −14.6 ± 1.8 V^{-1}. The shift in the voltage dependence, then, is a function of the membrane PD (this shift is shown later to vary according to the current through the channel) and varies from 15 to 38 mV over the experimental voltage range. This result reflects a negative surface PD at the cytoplasmic channel vestibule. The effect did not depend on whether NaCl or LiCl was used to adjust the ionic strength.

Voltage-dependent Ca^{2+} Block

Figure 4A shows the Ca^{2+} association rate, k^v_{on}; Fig. 4*B* shows the dissociation rate, k^v_{off} determined from the mean open and closed times in the presence of 20 mmol liter^{-1} Ca^{2+} (*see* Materials and Methods). The slope of the voltage dependence of k^v_{on} was not significantly (significance of 75%) altered by lowering the ionic strength of the cytoplasmic solution from 153 mmol liter^{-1} (17 patches; slope = −17.9 ± 1.4 V^{-1}) to approximately 5 mmol liter^{-1} (10 patches; slope = −19.7 ± 1.8 V^{-1}). However, this treatment did shift the voltage dependence of k^v_{on} by 17 ± 10 mV along the voltage axis. Adjusting the ionic strength with either NaCl, NH_4Cl, LiCl or $CaCl_2$ all produced the same result.

The voltage dependence of k^v_{off} (Fig. 4*B*) is more complex than that exhibited by k^v_{on} and k_c. The voltage dependence of $\log(k^v_{off})$ is nonlinear, particularly at low ionic strength. Similar results have been reported elsewhere (Neyton & Miller, 1988*a*; Laver, 1992) and have been attributed to the combined action of two dissociation mechanisms: one which operates mainly at smaller membrane PDs is Ca^{2+} dissociation to the vacuolar solution, and another which reverses the voltage dependence at extreme negative PD is Ca^{2+} dissociation to the cytoplasmic solution. It is the former that can be best determined over the experimental voltage range, so it is the shift in the voltage dependence of Ca^{2+} dissociation to the vacuolar solution that is measured here. This is determined from quadratic fits to the data at more positive membrane PDs. The results obtained from six patches exhibited a shift of 65 ± 15 mV when the ionic strength was reduced from 153 mmol liter^{-1} to approximately 5 mmol liter^{-1}. The shifts measured from an additional four patches (*data not shown*) were smaller and showed a greater variability (35 ± 25 mV).

The voltage dependence of k^v_{off} and k^v_{on} for vacuolar Ca^{2+} were found to depend on the ionic strength of the cytoplasmic solution only when it did not contain permeant ions. There was no ion species dependence in k^v_{off} for Na^+, NH_4^+, Li^+ or Ca^{2+} at either high or low ionic strength. Likewise the presence of the nonelectrolytes, sucrose, urea and mannitol had no significant effect on the blocking kinetics of Ca^{2+}.

Figure 5 shows the association k^c_{on} (Fig. 5*A*) and dissociation k^c_{off} rates (Fig. 5*B*) determined from the burst and gap durations in the presence of 1 mmol liter^{-1} cytoplasmic Ca^{2+} (*see* Materials and Methods). Reducing the ionic strength in the vacuolar solution from 153 mmol liter^{-1} to 4 mmol liter^{-1} produced no significant shift (10 ± 20 mV; significance of 75%) in k^c_{off} and only produced a slight shift (20 ± 18 mV; significance of 90%) in k^c_{on}. The surface potential in the vacuolar vestibule of the channel therefore appears to be too small to measure using this method.

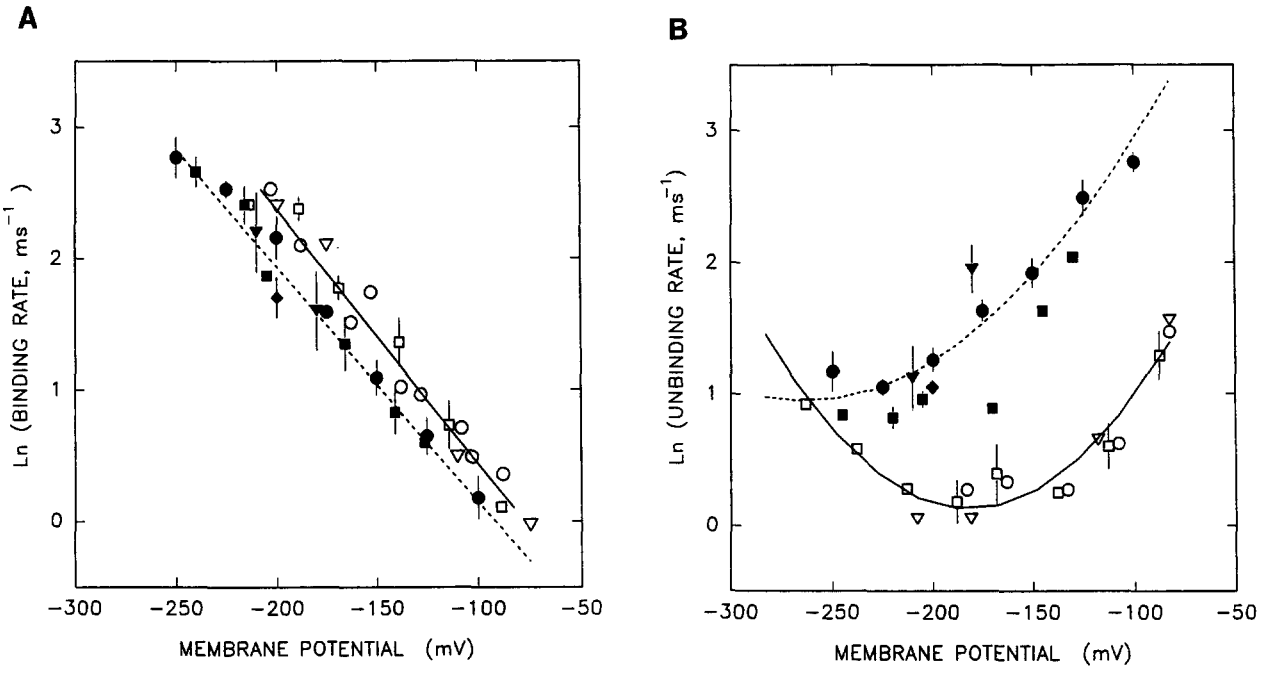

Fig. 4. The voltage-dependent binding kinetics of vacuolar Ca^{2+} in excised membrane patches in cytoplasmic solutions of low (open symbols) and high (filled symbols) ionic strength. The error bars represent the standard deviations of several measurements. The vacuolar solution contained 150 mmol liter^{-1} KCl + 20 mmol liter^{-1} $CaCl_2$. The cytoplasmic solutions contained (Symbol − concentrations (mmol liter^{-1}), # number of patches): (▽)-2 NaCl + 1 $CaCl_2$ + 300 sucrose, #1. (□)-2 $CaCl_2$, #4. (○)-2 $CaCl_2$ + 300 manitol, #1. (●)-150 NaCl + 2 or 5 $CaCl_2$, #11. (◆)-150 NH_4Cl + 1 $CaCl_2$, #2. (■)-150 LiCl + 5 $CaCl_2$, #2. (▼)-100 $CaCl_2$, #2. (*A*) The Ca^{2+} association rate determined from the channel mean open time (*see* Materials and Methods). Lowering the ionic strength shifts the kinetics 17 ± 10 mV along the voltage axis. This was determined from linear least-squares fits to the data in high (dashed line) and low (unbroken line) ionic strength. (*B*) The Ca^{2+} dissociation rate determined from the channel mean closed time within bursts (*see* Materials and Methods). The nonlinearity in voltage dependence of the Log (dissociation rate) is quite apparent in solutions of low ionic strength. Quadratic least-squares fits to the data obtained at high (dashed line) and low (unbroken line) ionic strength are shown. The 65 ± 15 mV shift in the kinetics is calculated from the data at low membrane PD where the quadratic curves are approximately parallel (*see* Discussion).

The Effect of Nonelectrolytes on Channel Conductance

The presence of nonelectrolytes that alter bulk viscosity in the bath solution is known to reduce channel conductance (Andersen, 1983; Laver et al., 1989). This effect has been interpreted as being a consequence of diffusion-limited ion flow through pores (*see* Introduction). To test this interpretation, the effects of nonelectrolytes on channel conductance in symmetric 1.5 mol liter^{-1} KCl were measured. The rationale for this is that at high [KCl], the channel conductance is only twofold larger than in 150 mmol liter^{-1} KCl (the channel saturates at high [KCl]), whereas the conductance of the electrolyte near the pore entrances should be approximately 10-fold higher. Thus, at high ion concentrations, ion flow is limited more by ion transport within the pore rather than by diffusion near the pore mouths. Therefore, the addition of nonelectrolytes should have a smaller attenuating effect at 1.5 mol liter^{-1} KCl than at 150 mmol liter^{-1} KCl. Our findings are that the symmetric addition of urea, sucrose, glycerol, ethylene glycol and mannitol all reduced channel conductance at both high and low [KCl]. The strongest attenuating effect was produced by 700 mmol liter^{-1} sucrose. This is shown in Fig. 6.

Discussion

Ion Binding or Screening?

In many instances when the ion composition of a medium affects membrane function, it is necessary to establish whether the observed effects result from ion binding or screening. Ion screening primarily involves long range electrostatic forces between mobile ions in the electrolyte and fixed charge sites on the channel protein. Electrostatic forces organize mobile ions so to mask, or screen, the presence of the fixed charge. Screening effects are relatively nonspecific and depend mainly on the valency of the mobile ions. Ion binding, however, involves short range interactions between molecules in

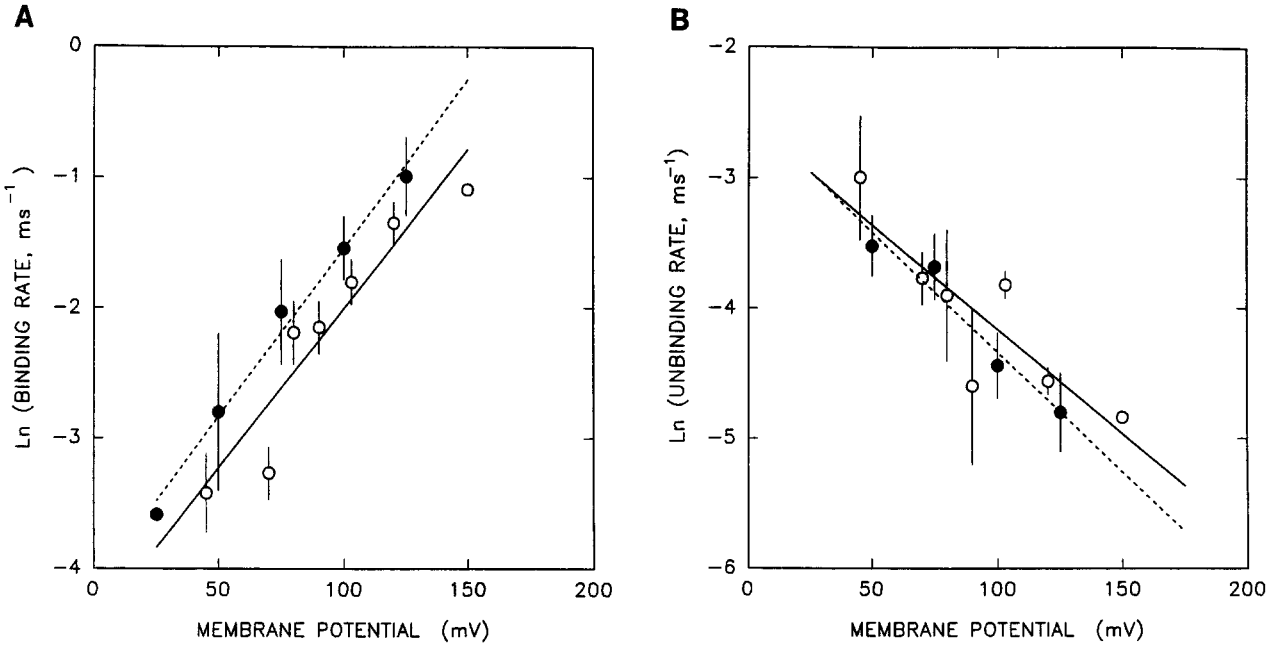

Fig. 5. The voltage-dependent binding kinetics of cytoplasmic Ca^{2+} in excised membrane patches in vacuolar solutions of low (open symbols) and high (filled symbols) ionic strength. The error bars represent the standard deviations of several measurements. The cytoplasmic solution contained 150 mmol liter^{-1} KCl + 1 mmol liter^{-1} $CaCl_2$. The vacuolar solutions contain (Symbol – concentrations (mmol liter^{-1}), # number of patches): (○)-1 $CaCl_2$ + 1 NaCl + 300 urea, #6. (●)-1 $CaCl_2$ + 150 NaCl, #6. (*A*) The Ca^{2+} association rate determined from the channel mean burst time (*see* Materials and Methods). There is only a marginal difference (20 ± 18) mV between the linear fits to the data obtained in low (unbroken line) and high (dashed line) ionic strength solutions. (*B*) The Ca^{2+} dissociation rate determined from the channel mean closed time between bursts (*see* Materials and Methods). Linear least-squares fits to the data show no significant difference (10 ± 20) mV between the data at high and low ionic strength.

which the hydration shells of the binding species are partly displaced (Eisenman, 1961). Consequently, the kinetics of ion binding is a specific property of each pair of binding species.

The validity of our analysis requires that the effects observed here are a consequence of ion screening. Since both ion screening and binding have been shown to produce similar effects on ion channel kinetics, it is important to determine whether the concentration-dependent shifts in channel kinetics arise from screening effects which yield information about pore mouth surface PDs or whether they arise from other mechanisms. Some examples of phenomena attributed to ion binding to maxi K channels are the effects of Na^+, Ba^{2+} and Ca^{2+} on channel gating (Miller, Latorre & Reisin, 1987; Laver, 1990; Neyton & Pelleschi, 1991), the effect of permeant ions on divalent ion block from the opposite side of the channel (Neyton & Miller, 1988*a,b;* Laver, 1992), and the biphasic concentration dependence of Ca^{2+} block in the *Chara* K^+ channel (Laver, 1992). Apparently, similar phenomena attributed to ion screening of maxi K channels are the biphasic concentration dependence of Mg^{2+} block and conductance *vs.* [KCl] (Bell & Miller, 1984; Moczydlowski et al., 1985; MacKinnon et al., 1989) and the shift in the voltage dependence of Ca^{2+} activation (MacKinnon et al., 1989).

A common way of distinguishing between ion screening and binding effects is to examine their ion specificity. According to this approach, phenomena which only depend on ionic strength result from a screening mechanism and those which depend on the ion species result from binding. This approach is adopted here. However, particular care must be exercised in the choice of ions used to vary the ionic strength. Ions permeable in maxi K channels such as K^+ and Rb^+ are notorious for altering the blocking kinetics of divalent ions (Neyton & Miller, 1988*a,b;* Laver, 1992) and toxins (Park & Miller, 1992; Toro, Stefani & Latorre, 1992) on the opposite side of the channel. They are also known to alter the kinetics of the channel's intrinsic gating mechanism (Neyton & Pelleschi, 1991). Relatively impermeant ions such as Na^+, Li^+ and NH_4^+ are used here because they are not known to have any species-specific effect on maxi K channels.

It is also the finding of this study that, in the absence of permeant ions, the kinetics of Gate A and vacuolar Ca^{2+} block was independent of which ion species was present both at high and low ionic strengths. More-

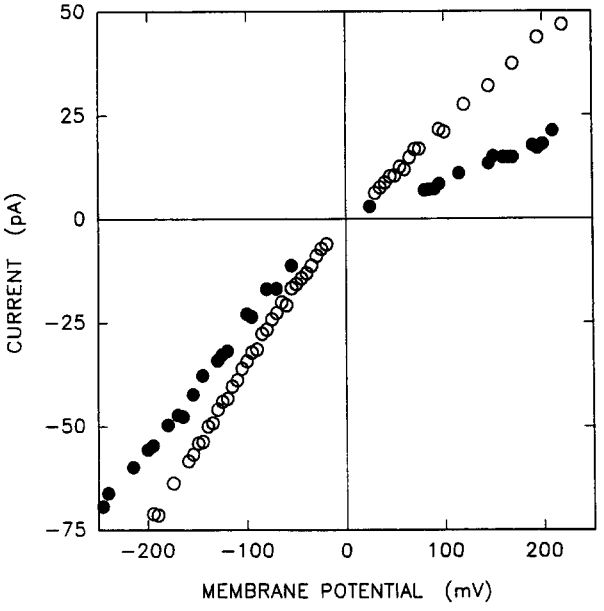

Fig. 6. The current-voltage characteristics of the channel from several excised patches bathed in symmetric solutions containing (○)-1.5 mol liter^{-1} KCl (three patches) and (●)-1.5 mol liter^{-1} KCl + 0.7 mol liter^{-1} sucrose (nine patches). These measurements were performed by forming a patch on the end of a pipette containing these solutions in a bath containing the normal bathing medium for the cytoplasmic drops. The patch is subsequently transferred to the measurement bath using the patch transfer technique of Quartararo and Barry (1987). Sucrose reduces the current at all membrane PDs and has its strongest effect at positive PD.

over, the presence of nonelectrolyte molecules had no effect on the channel kinetics. This is all consistent with a screening mechanism.

Further support for a screening mechanism comes from the ionic strength dependence of vacuolar Ca^{2+} block observed here being different from ion-specific effects reported previously for the permeant ions K^+ and Rb^+ (Laver, 1992). Raising the ionic strength increased the rate of Ca^{2+} dissociation and decreased its rate of association, whereas increasing either $[K^+]$ or $[Rb^+]$, keeping ionic strength constant with Na^+, increased only the Ca^{2+} dissociation rate. Another observation which relates to this is that the closing rate of Gate A, k_c, measured in drop-attached patches is significantly less than that from excised patches. The drop interior is known to contain the permeant ion K^+ (100 mmol liter^{-1}) and so it may be altering k_c by a mechanism like that described by Neyton and Pelleschi (1991).

Surface PD, Charge Density and Convergence Permeability Determined from Voltage Shifts

In the Theory section we explained that in the limit of infinite ionic strength the surface PD reduces to zero and the membrane PD is equal to the trans-pore PD. In the experimental situation, this is approximated using solutions with an ionic strength of about 150 mmol liter^{-1} where surface PDs are less than 5 mV and the membrane PD is likely to be within 5 mV of the trans-pore PD. Alternatively, lowering the ionic strength on either side of the membrane will produce a surface PD approximately equal to the shift in the voltage-dependent properties of the channel. From the surface PD, ionic strength and the current we can determine the charge density and convergence permeability at the pore entrance.

Figure 7 shows the current dependencies of both cytoplasmic (Fig. 7*A*) and vacuolar (Fig. 7*B*) surface PDs measured from shifts in voltage-dependent kinetics shown in Figs. 3–5 (ionic strength ~5 mmol liter^{-1}). Channel opening processes (Ca^{2+} dissociation) operate while no current flows and the channel closing processes (Ca^{2+} association and closing of Gate A) operate while there is current flow. In the latter case, the current is measured from amplitude of the closing transitions under conditions of low ionic strength on one side of the membrane. For example, in Fig. 7*A* values of surface PD (●) were taken from the data in Fig. 3 at membrane PDs of −50, −150 and −250 mV (with respect to the data at low ionic strength). The corresponding values of the current were also measured at these three membrane PDs.

We argue here that surface PDs measured using the different voltage-dependent channel properties vary exclusively according to the current. The current dependence is consistent with theoretical expectations and with the findings of an alternative method (*see below*). However, another explanation for the data could be that the voltage sensors for different processes have different locations within the channel protein and so would detect different local electric fields from the surface PD. The clearest evidence for a pure current dependence is derived from comparing surface PD estimates using the Ca^{2+} association and dissociation rates. This has an unambiguous interpretation because both processes operate at the one binding site (Laver, 1990). Consequently, there is very little difference between the two processes other than that Ca^{2+} dissociation operates while no current flows (the channel and surrounding electrolyte are in equilibrium) and Ca^{2+} association operates while there is current flow.

The charge densities are determined from the surface PD at zero current using Eq. (3). The convergence permeability is determined by fitting the observed current dependence of the surface PD with numerical solutions of the ion flux equations in the Appendix. The magnitude of charge density and convergence permeability so determined are listed in Table 1.

The cytoplasmic pore mouth possesses a surface charge (−0.035 C/m^2) of similar magnitude to that found on the maxi K channel in rat (~−0.01 C/m^2;

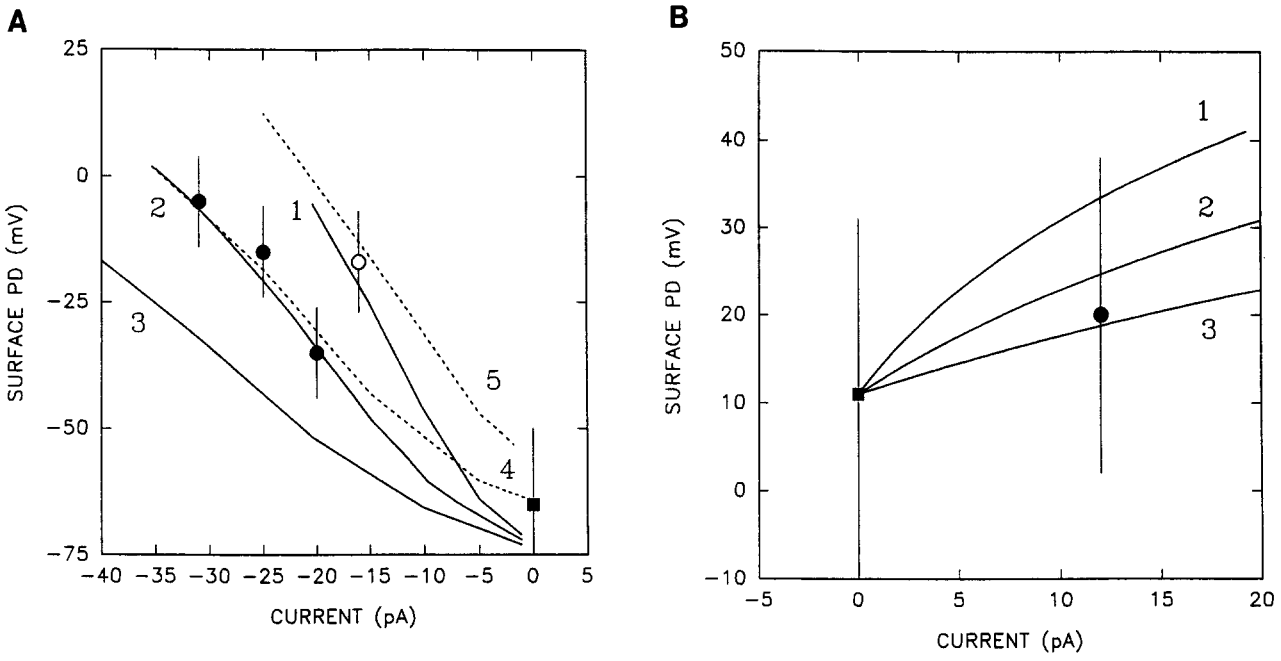

Fig. 7. The current-dependent surface PD at the cytoplasmic (*A*) and vacuolar (*B*) ends of the pore at low ionic strength determined from the results in Figs. 2–5. The lines show the numerical predictions of surface PD for the diffusion-limited, charged channel described in the Appendix. The charge densities and convergence permeabilities consistent with the data are listed in Table 1. (*A*) The surface PDs in 5 mmol liter^{-1} ionic strength cytoplasmic solutions determined from: (●)-the voltage-dependent gating, Gate A. (○)-Ca^{2+} association rate. (■)-Ca^{2+} dissociation rate. The unbroken lines were generated with $\Psi_0 = -74$ mV and show the effect of varying P_c where P_c ($\times 10^{-19}$ m^3/sec) = 0.65 (*1*); 1 (*2*); and 1.5 (*3*). The unbroken line, *3*, and the dashed lines show the effect of varying the surface charge density where $P_c = 1.5 \times 10^{-19}$ m^3/sec and $\Psi_0 = -74$ mV (*3*); −64 mV (*4*); and −54 mV (*5*). (*B*) The surface PDs in 4 mmol liter^{-1} ionic strength vacuolar solutions determined from: (●)-Ca^{2+} association rate. (■)-Ca^{2+} dissociation rate. The unbroken lines were generated with $\Psi_0 = 10$ mV and show the effect of varying P_c where P_c ($\times 10^{-19}$ m^3/sec) = 100 (*1*); 200 (*2*); and 400 (*3*).

Table 1. Estimates of charge density, σ, and convergence permeability, P_c, obtained from various sources for the K^+ channel in *Chara*

	Vacuolar side	Cytoplasmic side
$P_c \times 10^{-19} m^3/s$ (*a*)	>100	1.5 (1-3)
σ C/m^2 (*a*)	$(2 \pm 6) \times 10^{-3}$	$-(3.5 \pm 2) \times 10^{-2}$
σ C/m^2 (*b*)	$(0.4 \pm 0.6) \times 10^{-3}$	$-(1.2 \pm .1) \times 10^{-2}$
σ C/m^2 (*c*)	$(0 \pm 2) \times 10^{-3}$	

The charge densities were calculated from the zero-current surface PDs using Eq.(3). (*a*) P_c and σ determined from fitting ionic strength-dependent channel gating in Figs. 7*A* and *B* with the results of numerical calculations in the Appendix. (*b*) The charge density, σ, determined from fitting the K^+ permeation model (Eq. 5) with the unitary current data shown in Fig. 2*B*. The surface PDs at zero-current were derived from linear regression. (*c*) The charge density calculated from the voltage-dependent block of channel conductance by cytoplasmic Ca^{2+} at high and low ionic strength in the vacuolar solutions obtained from Laver (1992; Fig. 9*a*).

MacKinnon et al., 1989 and −0.05 C/m^2; Villarroel & Eisenman, 1989). However, the channels in *Chara* and rat differ in that the vacuolar pore mouth of the *Chara* channel is neutral, whereas in rat both ends of the pore have substantial negative charge density. When the values for the convergence permeabilities are compared with the intrinsic permeability of the channel (~10^{-17} m^3/sec; Laver et al., 1989) it can be seen that the convergence permeability of the cytoplasmic solution is much lower than either that of the vacuolar solution or the channel itself. Hence, the properties of the cytoplasmic pore mouth are the most important factors determining the overall conductance of the channel-electrolyte system. The consequences of these findings are elaborated below (*see* Re-evaluation of the K^+ Permeation Model).

Surface PD, Charge Density and Convergence Permeability Determined from Mg^{2+} Block

In the previous section, the surface PD measurements were made using the "tilt effect" model where the transpore PD was probed using channel block by ions which do not in themselves contribute significantly to the ionic strength of the electrolyte and so do little to screen surface PDs. Another method (Moczydlowski et al., 1985; MacKinnon et al., 1989) measures block by ions that also contribute to a large component of the ionic

Table 2. Summary of the analysis of Mg^{2+} block

	Vacuolar side				Cytoplasmic side				
Membrane PD (mV)	−25	0	25	50	−75	−50	−25	0	25
K_D for Mg^{2+} (mmol liter^{-1})	3	4	6	9	28	14	8	5	4
$I(0)$ (pA)	4.5	6.8	8.5	10	−13	−11	−9	−7	−5
Surface PD (mV)	20	25	33	39	25	10	−10	−20	−33

Parameters used to fit the data in Fig. 2*B* using Eq.(5) are summarized above.

strength and so are themselves involved in screening. Here, Mg^{2+} block of K^+ conductance is measured at low ionic strength. The results are interpreted in terms of the "tilt" model using the following equation (Eq. 5) from MacKinnon et al. (1989).

$$I([Mg^{2+}]) = \left\{ I(0) + \frac{GRT}{F}\left[\Psi(0) - \Psi([Mg^{2+}])\right]\right\} \cdot \left\{1 + \frac{[Mg^{2+}]}{K_D}\exp\left[-2\Psi([Mg^{2+}])\right]\right\} \quad (5)$$

where G is the conductance of the channel which is 90 to 100 pS under these conditions and Ψ is the $[Mg^{2+}]$-dependent, i.e., ionic strength-dependent, surface PD. The first term on the right side of Eq. (5) represents the shift in the current-voltage characteristic due to the tilt effect. The second term allows for the voltage-dependent block of the channel by Mg^{2+}. The equation is only valid when permeant ions are present only on one side of the membrane (here $[K^+]$ = 150 mmol liter^{-1}), i.e., the ion flow must be unidirectional. In these experiments, there was also a small amount of K^+ present on the other side of the membrane (3 mmol liter^{-1}). However, this concentration was too low to significantly affect the current-voltage properties of the channel.

Equation (5) is fitted with the data shown in Fig. 2*B* and the parameters of the fit are given in Table 2 and graphed in Fig. 8. The current dependence of Ψ^v and Ψ^c shown in Fig. 8 is similar to that derived from the channel gating kinetics shown in Fig. 7. The zero-current intercept is equal to Ψ_0 and the slope gives a measure of the degree of diffusion limitation. Thus Ψ_0 at the cytoplasmic side, in 3 mmol liter^{-1} KCl, is (−71 ± 8) mV and on the vacuolar side it is (3 ± 6) mV. The corresponding surface charge densities, calculated using Eq. (3) are $-(1.2 \pm 0.1) \times 10^{-2}$ and $(0.4 \pm 0.6) \times 10^{-3}$ C/m^2, respectively. The stronger current dependence of the cytoplasmic surface PD indicates that the cytoplasmic entrance to the pore has the lower convergence permeability.

A novel feature of the data in Fig. 2 is that at more negative membrane PDs the blocking effect of Mg^{2+} is reversed i.e., the current is enhanced. This can be understood in terms of the combined effects of surface charge and diffusion-limited ion flow on the electrostatic potential and $[K^+]$ near the pore as follows (*see* Fig. 1). At a small membrane PD, the current is also small and the negative surface PD results mainly from the negative fixed charge. A negative potential attracts K^+ to the pore entrance causing an increase in channel conductance. Screening the potential then decreases the pore conductance. However, at more extreme membrane PDs where the current is large, the surface PD becomes positive. Thus, screening of the potential by Mg^{2+} has the opposite effect. The driving force on ions within the pore is also affected by Mg^{2+}. At low ionic strength, a large fraction of the membrane PD actually appears across the cytoplasmic solution near the pore mouth and not the pore. Screening surface PD by the addition of Mg^{2+} enhances the current by increas-

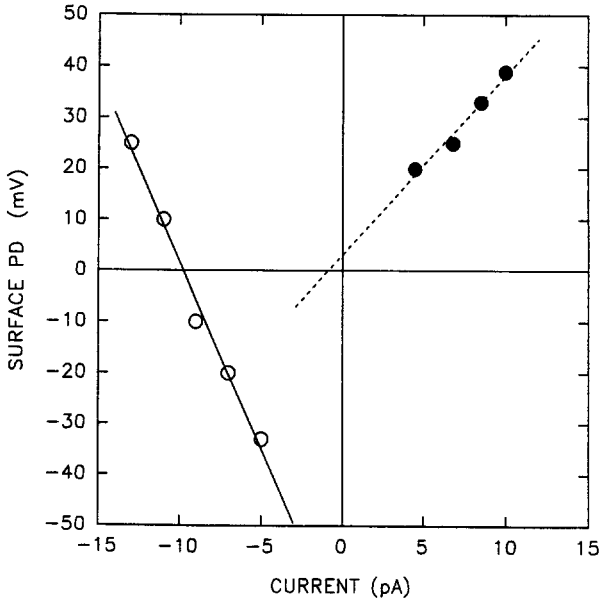

Fig. 8. The current-dependent surface PD at the cytoplasmic (○) and vacuolar (●) ends of the pore at low ionic strength determined from the data in Fig. 2*B*. The zero-current surface PDs, obtained from linear regression of the data are (−71 ± 8) mV for the cytoplasmic side (unbroken line) and (3 ± 6) mV for the vacuolar side (dashed line). The charge densities, calculated from these values using Eq. (3), are listed in Table 1.

ing the proportion of the membrane PD that appears across the pore itself.

Experimental Scatter

In most cases the channel kinetics depended on ionic strength and current as shown in Figs. 3 and 4. However, in a few instances a decrease in the ionic strength of the bathing medium produced a smaller-than-usual shift in the voltage-dependent kinetics of the channel (*see* Results). This is most likely due to the formation of a membrane vesicle, instead of an inside-out patch, on the patch electrode during excision. A vesicle would occlude the cytoplasmic side of the channel from the bath and so it would not get full exposure to solutions of low ionic strength.

An alternative, though less likely interpretation of the experimental scatter, would be that we are studying a heterogeneous population of channels where there are variations in charge density near the pore entrances. If this were so, then channels with smaller charge densities would also have smaller convergence permeabilities (*see* Theory) and so would be more severely diffusion limited. This in turn would lead to an increase in the current dependence in the measured surface PDs. The data showed the opposite effect, i.e., channels with weaker ionic strength dependence also showed weaker current dependence.

Re-evaluation of the K^+ Permeation Model for the *Chara* Channel

The model for K^+ permeation in the maxi K channel in *Chara* proposed by Laver et al. (1989) and Laver (1990) has four tenets. These are re-evaluated here in the light of the data presented in this study.

(*1*) *Electrodiffusion Approximation*

It was assumed that the permeation of ions through the pore is described by the Goldman-Hodgkin-Katz equation. The proposed transport process underlying this equation is that ions cross the channel by passing a large number ($n > 5$) of uniform energy barriers (Läuger, 1973; *see also* Eisenman & Horn, 1983; Barry & Gage, 1984). Consequently, in symmetrical solutions that contain no blocking ions, the *I-V* characteristic of the channel must be linear. In previous studies, nonlinear and asymmetric *I-V* data were attributed to the effects of diffusion limitation and surface charge. The data shown in Fig. 6 were obtained from a channel in symmetric 1.5 mol liter^{-1} KCl where the effects of diffusion limitation and surface charge are small (*see below*). Under these conditions, the *I-V* characteristic is nonlinear and asymmetric so it appears that electrodiffusion cannot accurately account for these data. We have found that modeling the ion permeation pathway with three sequential energy barriers provides a much better fit to the data over a range of [KCl] from 0.3 to 2 mol liter^{-1} (D.R. Laver, *unpublished data*). Therefore, a multi-barrier (possibly three barriers) model rather than an electrodiffusion model should be used to explain the permeation characteristics of this channel. Multi-barrier models have been successfully used elsewhere to explain K^+ permeation in maxi K channels (*see articles cited in* Hägglund, Eisenman & Sandblom, 1984).

(*2*) *"Single-Ion" Conduction*

K^+ transport in the *Chara* channel was modeled using the assumption that only one ion occupies the pore at any time, i.e, "single ion" conduction. Consequently, K^+ permeation is described by Michaelis-Menten kinetics. However, it has been shown that K^+ transport in maxi K channels obeys multi-ion kinetics (Neyton & Miller, 1988*a,b;* Laver, 1992) and so will deviate from Michaelis-Menten kinetics. Laver (1992) presented evidence for four K^+ binding sites within the channel of which two were characterized. A specific "multi-ion" model for K^+ permeation in this channel has not yet been developed and so in the absence of such a model a "single-ion" approximation must suffice, so values of ion binding parameters as well as σ determined from fitting the Mg^{2+} block with this model represent qualitative estimates. Studies of the blocking effect of monovalent cations such as Cs^+ on the conductance of the maxi K channel from animal tissue have led to the proposal of detailed multi-ion models (Yellen, 1984*a,b;* Eisenman, Latorre & Miller, 1986; Cecchi et al., 1987). Similar studies still need to be done with the *Chara* maxi K channel.

(*3*) *Diffusion-limited Ion Flow*

Laver (1990) proposed that the electrolyte at both ends of the pore significantly limited transport of K^+ through the maxi K channel. Diffusion limitation explained the sublinear and asymmetric nature of the *I-V* data as well as the attenuating effect of sucrose on channel conductance. The sucrose effect was believed to occur via an increased viscosity of the electrolyte near the pore mouths. Ions diffuse more slowly in viscous media, so increasing the bulk viscosity with sucrose should decrease the convergence permeability. It was anticipated that the molecular dimensions of sucrose precluded it from entering the pore so that it would not alter the intrinsic permeability of the channel. A prediction of this model is that addition of sucrose (0.7 mol liter^{-1}) will produce less than a 10% reduction in current when

[KCl] is 1.5 mol liter^{-1}. It is clear from the data in Fig. 6 that the symmetric addition of sucrose has a much stronger effect than this. Figure 9 shows that the attenuating effect of a variety of nonelectrolytes on the current at 150 mV is closely correlated with their effects on bulk viscosity. It appears that these molecules exert their effect by altering the ion transport process within the pore rather than near the pore mouths and that altering bulk viscosity is a poor test for diffusion-limited ion flow.

The main advance that this study makes in addressing the question of diffusion limitation is that the surface PD is used to probe diffusion-limited flow. The surface PD approach indicates that the electrolyte outside the cytoplasmic entrance of the channel significantly limits K^+ current. This is consistent with the results of modeling the voltage-dependent Mg^{2+} block. The findings presented here contradict some of the previous findings of Laver et al. (1989) where it was also proposed that ion diffusion in the vacuolar solution limits the channel current. Their interpretation was based on the attenuating effects of sucrose on the current which has now been discredited (*see above*).

(*4*) *Negative Charges Fixed near the Pore Entrances*

The presence of net charge at the pore entrances of the *Chara* K^+ channel was invoked to account for the relative increase in its intrinsic and convergence permeabilities at low ionic strength (Laver et al., 1989). This study provides direct evidence for the presence of negative charge fixed at the cytoplasmic entrance to the channel. Table 1 shows estimates of the charge densities obtained from three sources, namely, (1) the ionic strength dependence of channel gating and the Ca^{2+} association and dissociation rates (*see* Figs. 5–7); (2) cytoplasmic Ca^{2+} block presented by Laver (1992; Fig. 9*a*); and (3) the Mg^{2+} block of the unitary current. All the measurements gave a consistent picture of the charge distribution on the channel in which the charge density at the vacuolar channel entrance is at least an order of magnitude smaller than that for the cytoplasmic side.

There is enough negative charge on the cytoplasmic side of the pore to significantly enhance K^+ permeation at physiological ion concentrations. Fluctuations in surface charge density have been proposed as a mechanism for conductance substates in this channel (Tyerman, Findlay & Terry, 1992). The results presented here indicate that neutralization of fixed charges at the cytoplasmic end of the pore is a feasible mechanism for conductance substates.

Conclusions

All experimental approaches used here give a consistent picture of permeation in the *Chara* maxi K channel in which the surface charge and convergence permeability of the cytoplasmic vestibule are the major factors in determining channel conductance.

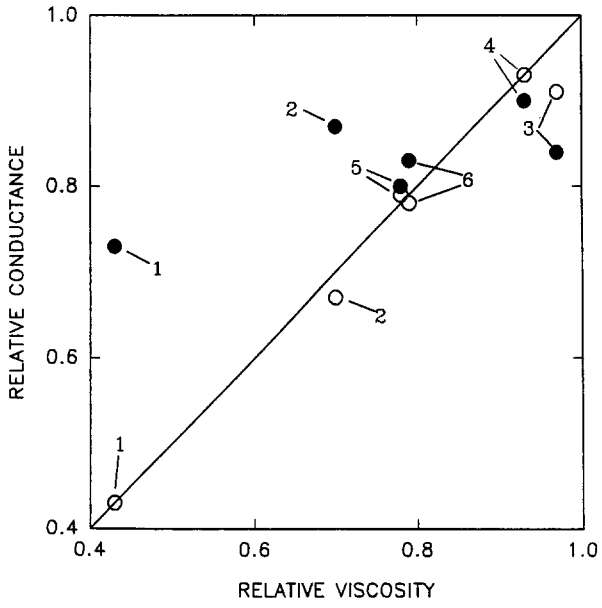

Fig. 9. The relationship between bulk viscosity of the electrolyte and the chord conductance of the maxi K channel from *Chara* in symmetric solutions containing 1.5 mol liter^{-1} KCl. The open symbols are relative conductances at a membrane PD of +150 mV and filled symbols are those at −150 mV. The viscosity was increased by the symmetric addition of nonelectrolytes to the vacuolar and cytoplasmic baths. The numbers indicate the presence of the following: (*1*) sucrose, 0.7 mol liter^{-1}; (*2*) sucrose, 0.35 mol liter^{-1}; (*3*) urea, 0.75 mol liter^{-1}; (*4*) ethylene glycol 1.6 mol liter^{-1}; (*5*) ethylene glycol 0.5 mol liter^{-1}; (*6*) glucose 0.5 mol liter^{-1}.

The cytoplasmic vestibule of the *Chara* channel has a charge density of −0.035 C/m^2 which is similar to that found in maxi K channels from rat muscle. The properties of the vacuolar vestibule, which is effectively neutral, differ from the negatively charged external vestibules in rat maxi K channels indicating differing protein structures in this part of the channel.

The surface PD at the cytoplasmic vestibule depends on the current through the channel. This can be understood in terms of diffusion-limited ion flow, where the relatively low convergence permeability outside the cytoplasmic vestibule is a major determinant of the channel conductance. The surface PD at the vacuolar vestibule does not depend on the current, indicating that the convergence permeability outside the vacuolar vestibule is relatively high and does not contribute significantly to the channel conductance.

The addition of nonelectrolytes such as sucrose to the bathing solutions is a poor test for the significance of diffusion-limitation effects. It appears that these molecules alter channel conductance by interfering with the intrinsic permeation mechanism of the channel

rather than by altering bulk viscosity. A much better approach to testing for diffusion-limited ion flow is to measure the dependence of the surface PD on the current passing through the channel.

We wish to thank Dr. N.A. Walker and Dr. P.W. Gage for critically reading this manuscript. This work was supported by an ARC Queen Elizabeth II Fellowship.

References

Andersen, O.S. 1983. Ion movement through gramicidin A channels: Studies on the diffusion-controlled association step. *Biophys. J.* **41:**147–165

Apell, H.-J., Bamberg, E., Alpes, H., Läuger, P. 1977. Formation of ion channels by a negatively charged analog of gramicidin. *J. Membrane Biol.* **31:**171–188

Apell, H.-J., Bamberg, E., Läuger, P. 1979. Effects of surface charge on the conductance of the gramicidin channel. *Biochim. Biophys. Acta* **552:**369–378

Barry, P.H., Gage, P.W. 1984. Ion selectivity of channels at the endplate. W.D. Stein, editor. *In:* Current Topics in Membranes and Transport. Volume 21, pp. 1–51. Academic, NY

Barry, P.H., Lynch, J.W. 1991. Liquid junction potentials and small cell effects in patch-clamp analysis. *J. Membrane Biol.* **121:**101–117

Bell, J., Miller, C. 1984. Effects of phospholipid surface charge on ion conduction in the K^+ channel of sarcoplasmic reticulum. *Biophys. J.* **45:**279–287

Blatz, A.L., Magleby, K.L. 1986. Correcting single channel data for missed events. *Biophys. J.* **49:**967–980

Dani, J.A. 1986. Ion-channel entrances influence permeation. Net charge, size, shape, and binding considerations. *Biophys. J.* **49:**607–618

Decker, E.R., Levitt, D.G. 1988. Use of weak acids to determine the bulk diffusion limitation of H^+ ion conductance through the gramicidin channel. *Biophys. J.* **53:**25–32

Eberl, M. 1993. Electrodiffusion in Electrolytes and Membranes. Ph.D. thesis. University of New South Wales, Australia

Eisenman, G. 1961. On the elementary atomic origin of equilibrium ionic specificity. *In:* Symposium on Membrane Transport and Metabolism. A. Kleinzeller and A. Kotyk, editors. pp. 163–179. Academic, New York

Eisenman, G., Horn, R. 1983. Ionic selectivity revisited: The role of kinetic equilibrium processes in ion permeation through channels. *J. Membrane Biol.* **76:**197–225

Eisenman, G., Latorre, R., Miller, C. 1986. Multi-ion conduction and selectivity in the high-conductance Ca^{++}-activated K^+ channel from skeletal muscle. *Biophys. J.* **50:**1025–1034

George, E.P., Simons, R. 1966. Solutions of the field equations in the fixed-charge model of cell membranes. *Aust. J. Biol. Sci.* **19:**459–470

Gilbert, D.L., Ehrenstein, G. 1984. Membrane surface charge. *Curr. Top. Membr. Trans.* **22:**407–421

Green, W.N., Andersen, O.S. 1991. Surface charges and ion channel function. *Annu. Rev. Physiol.* **53:**341–359

Grahame, D. 1947. The electrical double layer and the theory of electrocapillarity. *Chem. Rev.* **41:**441–501

Hägglund, J.V., Eisenman, G., Sandblom, J.P. 1984. Single-salt behaviour of a symmetrical 4-site channel with barriers at its middle and ends. *Bull. Math. Biol.* **46:**41–80

Imoto, K., Busch, C., Sakmann, B., Mishina, M., Konno, T., Nakai, J., Bujo, H., Mori, Y., Fukuda, K., Numa, S. 1988. Rings of negatively charged amino acids determining the acetylcholine receptor channel conductance. *Nature* **335:**645–648

Jordan, P.C. 1987. How pore mouth charge distributions alter the permeability of transmembrane ionic channels. *Biophys. J.* **51:**297–311

Kamiya, N., Kuroda, K. 1957. Cell operation in *Nitella:* I. Cell amputation and effusion of the endoplasm. *Proc. Japan. Acad.* **33:**149–152

Latorre, R., Miller, C. 1983. Conduction and selectivity in potassium channels. *J. Membrane Biol.* **71:**11–30

Läuger, P. 1973. Ion transport through pores: a rate-theory analysis. *Biophys. Biochim. Acta* **311:**423–441

Läuger, P. 1976. Diffusion-limited ion flow through pores. *Biophys. Biochim. Acta* **455:**493–509

Laver, D.R. 1990. Coupling of K^+-gating and permeation with Ca^{2+} block in the Ca^{2+}-activated K^+ channel in *Chara australis. J. Membrane Biol.* **118:**55–67

Laver, D.R. 1992. Divalent cation block and competition between divalent and monovalent cations in the large-conductance K^+ channel from *Chara australis. J. Gen. Physiol.* **100:**269–300

Laver, D.R., Fairley, K.A., Walker, N.A. 1989. Ion permeation in a K^+ channel in *Chara australis:* Direct evidence for diffusion limitation of ion flow in a maxi-K channel. *J. Membrane Biol.* **108:**153–164

Laver, D.R., Walker, N.A. 1987. Steady-state voltage-dependent gating and conduction kinetics of single K^+ channels in the membrane of cytoplasmic drops of *Chara australis. J. Membrane Biol.* **100:**31–42

Laver, D.R., Walker, N.A. 1991. Activation by Ca^{2+} and block by divalent ions of the K^+ channel in the membrane of cytoplasmic drops from *Chara australis. J. Membrane Biol.* **120:**131–139

Levitt, D.G. 1985. Strong electrolyte continuum theory solution for equilibrium profiles, diffusion limitation, and conductance in charged ion channels. *Biophys. J.* **48:**19–31

Levitt, D.G. 1991. General continuum theory for multiion channel. II. Application to acetylcholine channel. *Biophys. J.* **59:**278–288

MacKinnon, R., Latorre, R., Miller, C. 1989. Role of electrostatics in the operation of a high-conductance Ca^{2+}-activated K^+ channel. *Biochemistry* **28:**8092–8099

MacKinnon, R., Miller, C. 1989. Functional modification of a Ca^{2+}-activated K^+ channel by trimethyloxonium. *Biochemistry* **28:**8087–8092

Margolis, M.J. 1966. Chemical Principles in Calculation of Ionic Equilibria. Macmillan, New York

Miller, C., Latorre, A., Reisin, I. 1987. Coupling of voltage-dependent gating and Ba^{++} block in the high conductance Ca^{++}-activated K^+ channel. *J. Gen. Physiol.* **90:**427–449

Moczydlowski, E., Alvarez, O., Vergara, C., Latorre, R. 1985. Effect of phospholipid surface charge on the conductance and gating of a Ca^{2+}-activated channel in planar lipid bilayers. *J. Membrane Biol.* **83:**273–282

Neyton, J., Miller, C. 1988*a*. Potassium blocks barium permeation through the high conductance Ca^{2+}-activated K^+ channel. *J. Gen. Physiol.* **92:**549–567

Neyton, J., Miller, C. 1988*b*. Discrete Ba^{2+} block as a probe of ion occupancy and pore structure in the high conductance Ca^{2+}-activated K^+ channel. *J. Gen. Physiol.* **92:**569–586

Neyton, J., Pelleschi, M. 1991. Multi-ion occupancy alters gating in high-conductance, Ca^{2+}-activated K^+ channels. *J. Gen. Physiol.* **97:**641–665

Park, C.S., Miller, C. 1992. Interaction of charybdotoxin with permeant ions inside the pore of a K^+ channel. *Neuron* **9:**307–313

Peskoff, A., Bers, D.M. 1988. Electrodiffusion of ions approaching

the mouth of a conducting membrane channel. *Biophys. J.* **53**:863–875

Quartararo, N., Barry, P.H. 1987. A simple technique for transferring excised patches of membrane to different solutions for single-channel measurements. *Pfluegers Arch.* **410**:677–678

Toro, L., Stefani, E., Latorre, R. 1992. Internal blockade of a Ca^{2+}-activated K^+ channel by Shaker B inactivating "ball" peptide. *Neuron* **9**:237–245

Tyerman, S.D., Findlay, G.P., Terry, B.R. 1992. Behaviour of K^+ and Cl^- channels in the cytoplasmic drop membrane of *Chara corallina* using a transient detection method of analysing single-channel recording. *Biophys. J.* **61**:736–749

Villarroel, A., Eisenman, G. 1989. Ca^{2+} block in the large Ca^{++}-activated K^+ channel: An estimate of the surface charge of the internal vestibule. *Biophys. J.* **55**:7*a* (*Abstr.*).

Ximena, C., Wolff, D., Alvarez, O., Latorre, R. 1987. Mechanisms of Cs^+ blockade in a Ca^{2+}-activated K^+ channel from smooth muscle. *Biophys. J.* **52**:707–716

Yellen, G. 1984*a*. Ionic permeation and blockage in Ca^{2+}-activated K^+ channels of bovine chromaffin cells. *J. Gen. Physiol.* **84**:157–186

Yellen, G. 1984*b*. Relief of Na^+ block of Ca^{2+}-activated K^+ channels by external cations. *J. Gen. Physiol.* **84**:187–199

Appendix

Introduction

When the permeability of an ion channel is high compared with that of the adjacent aqueous phases the ion transport rate becomes limited by the rate of diffusion of ions to and from the pore entrances (or aqueous convergence regions). Läuger (1976) provided the first rigorous theoretical treatment of diffusion-limited ion flow through a neutral, cylindrical pore, where the ends of the pore act as a hemispherical sink or source of permeant ions. The properties of the aqueous convergence regions are summarized by their convergence permeability, P_c. The observed channel conductivity is the series combination of the two aqueous convergence regions and the channel interior (permeability = P_i). More recently Peskoff and Bers (1988) presented several approximate analytical relationships describing electrodiffusion of ions near the mouths of charged pores. The effect of fixed charges on diffusion limitation has also been considered by Latorre and Miller (1983), Levitt (1985), Jordan (1987) and Decker and Levitt (1988). Ion permeation models specific to particular ion channels with known structures, such as the acetylcholine receptor channel, also include the effects of fixed charges (e.g., Dani, 1986; Levitt, 1991). These studies find that fixed charge at the entrance of ion channels increases their convergence permeability to counter ions. Although exact analytic solutions for the small signal, a.c. impedance of diffusion-limited pores have recently been published (Eberl, 1993), no such solutions exist for the steady-state case.

The main body of this paper is concerned with determining the surface PD of the K^+ channel in *Chara* and its dependence on the current. The Appendix describes the method by which the theoretical relationship between current and pore mouth surface PD is calculated for a range of surface charge densities and convergence permeabilities. The numerical results are compared with the experimental data in Fig. 7.

Method

Ions are considered to diffuse radially from the pore entrance defined by a hemisphere of radius r_0. The flux J_k of each ion species, k, is related to the permeability of the pore P_i and the aqueous convergence regions, P_c, by the Nernst-Planck equation (Eqs. A1–A3 and A5–A7). Poisson's equation (Eqs. A4 and A9) relates the space charge to the electric field, E. The three ion species considered here, with concentrations C_k, are monovalent, permeant cations ($k = 1$), impermeant divalent cations ($k = 3$) and a common monovalent anion species ($k = 2$). The equations are solved in spherical coordinates ($r_0 \le r \le \infty$) on each side of the membrane (Eqs. A1–A4) and within the membrane cartesian coordinates ($-L/2 \le x \le L/2$) are used (Eqs. A5–A8).

$$\frac{J_1}{P_c(r^2/r_0)} = \frac{dC_1}{dr} + C_1E \tag{A1}$$

$$\frac{J_2}{P_c(r^2/r_0)} = \frac{dC_2}{dr} - C_2E \tag{A2}$$

$$\frac{J_3}{P_c(r^2/r_0)} = \frac{dC_3}{dr} + 2C_3E \tag{A3}$$

$$\frac{1}{r^2}\left(\frac{d}{dr}(r^2E)\right) = \frac{-FQ}{\varepsilon_0\varepsilon_r} \tag{A4}$$

$$P_c \equiv 2\pi r_0 D$$

$$\frac{J_1}{P_i} = \frac{dC_1}{dx} + C_1E \tag{A5}$$

$$\frac{J_2}{P_i \times 10^{-4}} = \frac{dC_2}{dx} - C_2E \tag{A6}$$

$$\frac{J_3}{P_i \times 10^{-4}} = \frac{dC_3}{dx} + 2C_3E \tag{A7}$$

$$\frac{dE}{dx} = \frac{-FQ}{\varepsilon_0\varepsilon_r} \tag{A8}$$

$$P_i \equiv AD/L$$

where D is the ion diffusion coefficient, FQ is the net charge concentration and $Q = C_1 - C_2 + 2C_3 + C_f$. The fixed charges are considered to be homogeneously distributed with a concentration C_f over regions bounded by $r_0 \le r \le r_\sigma$ and zero elsewhere. The electric potential V is in units of RT/F. Positive flux is defined as ions flowing away from the pore.

The general approach to solving these equations is the same as that used by George and Simons (1966). The equations are integrated numerically using a step size of $\lambda/400$ (λ is the Debye length) starting at $r = 15\lambda$ and ending at the pore midplane, $x = 0$. The fundamental difficulty with the integration procedure is that the boundary conditions are only specified at $r = \infty$. Merely setting the variables, Q and E to zero at some large value of r leads to large errors because they are amplified with each numerical interaction. This problem is overcome by approximating the boundary conditions by an asymptotic expansion of $\Phi(r)$, the electric potential, $E(r)$ and ion concentrations for large r. Peskoff and Bers (1988) presented the asymptotic solution for the case of monovalent electrolytes. Briefly, the Nernst-Planck and Poisson equations were combined to produce a single integro-differential equation. The logarithm of the electrostatic potential at large r was replaced with a series expansion in terms of $1/r$. The coefficients of the expansion, a_i, were obtained by equating terms of the same order. The asymptotic solution for the more complicated case when electrolytes contain both monovalent and divalent cations

is derived here by the same method. The ion concentrations are re-expressed in terms of η to simplify the equations:

$$C_1 = \eta C\,; \quad C_2 = C\,; \quad C_3 = \frac{(1-\eta)}{2} C$$

Thus when $r >> \lambda$ and $r >> r_0$

$$\Phi(r) \to \Phi(\infty)(1+n)$$

$$E(r) \to \frac{-a_1 N - 2a_2 N^2 - 3a_3 N^3 - 4a_4 N^4 - 5a_5 N^5}{r(1+n)}$$

$$C_1(r) \to \eta C(1+n)$$

$$C_2(r) \to C/(1+n)$$

$$C_3(r) \to \frac{(1-\eta)}{2} C(1+n)^2$$

$$Q(r) \to \frac{C(4N\lambda)^2\eta}{r^2(\eta-3)^3} + \frac{32N^3(9-9\eta-9\eta^2)\lambda^2}{r^2(\eta-3)^5}$$

where $n = a_1 N + a_2 N^2 + a_3 N^3 + a_4 N^4 + a_5 N^5$

$$a_1 = \frac{2}{\eta - 3}$$

$$a_2 = \frac{6(\eta-1)}{(\eta-3)^3} + \frac{16\eta\lambda^2}{(\eta-3)^4}$$

$$a_3 = \frac{4(\eta-1)(5\eta+3)}{(\eta-3)^5} + \frac{288(3-\eta-4\eta^2)\lambda^2}{5(\eta-3)^6}$$

$$a_4 = \frac{10(\eta-1)(\eta+3)(7\eta-3)}{(\eta-3)^7}$$

$$a_5 = \frac{12(\eta-1)(-45-33\eta+121\eta^2+21\eta^3)}{(\eta-3)^9}$$

$$N \equiv \frac{-J}{4\pi DCr} \quad \text{and} \quad \lambda \equiv \sqrt{\frac{\varepsilon_0 \varepsilon_r RT}{2F^2 C}}$$

where λ is the Debye length and N is a constant. Thus, at large r the variables E, Q and C on each side of the pore are related by the one parameter, N. Numerical solutions for a given value of J_1 are obtained by slightly adjusting the values of N on each side of the pore as well as J_2 and J_3 such that integrating the equations on both sides of the midplane produce matching values of E, Q, C_1, C_2 and C_3 at $x = 0$ (tolerance of better than 0.1%). To match all these parameters at the pore midplane, it is necessary that the impermeant ions have a small, but finite permeability in the pore. Here, the relative permeabilities for "impermeant" ions were set to 10^{-4}.

The electrostatic potential difference between the right entrance to the pore and that at $r = \infty$ (i.e., the surface PD; *see* Fig. 1) was calculated as a function of the current for several values of the convergence permeability and surface charge density. The results for the case when the electrolyte on the right of the channel contains 2 mmol liter^{-1} $MgCl_2$ plus 0.1 mmol liter^{-1} KCl and on the left contains 100 mmol liter^{-1} KCl are shown in Fig. 7. The current-dependent component of the surface PD, Ψ_p, is approximately inversely proportional to P_c and increases with decreasing surface charge density at the channel vestibule.